



Published in final edited form as:

Shock. 2016 October ; 46(4): 431–438. doi:10.1097/SHK.0000000000000611.

Neutralization of Osteopontin Ameliorates Acute Lung Injury Induced by Intestinal Ischemia-Reperfusion

Yohei Hirano, MD^{1,3}, Monowar Aziz, PhD¹, Weng-Lang Yang, PhD^{1,2}, Mahendar Ochani, MD¹, and Ping Wang, MD^{1,2}

Yohei Hirano: Yhirano@northwell.edu; Monowar Aziz: Mazizl@northwell.edu; Weng-Lang Yang: WLYang@northwell.edu; Mahendar Ochani: MOchani@northwell.edu; Ping Wang: Pwang@northwell.edu

¹Center for Translational Research, The Feinstein Institute for Medical Research, Manhasset, New York, United States

²Department of Surgery, Hofstra Northwell School of Medicine Manhasset, New York, United States

³Department of Emergency and Critical Care Medicine, Juntendo University, Urayasu Hospital, Urayasu, Chiba, Japan

Abstract

Intestinal ischemia-reperfusion (I/R) is associated with acute respiratory distress syndrome (ARDS). Osteopontin (OPN), a glycoprotein secreted from immune-reactive cells, plays a deleterious role in various inflammatory diseases. Considering OPN as a pro-inflammatory molecule, we hypothesize that the treatment with its neutralizing antibody (anti-OPN Ab) protects mice against intestinal I/R-induced acute lung injury (ALI). Intestinal I/R was induced in mice by superior mesenteric artery (SMA) occlusion with a vascular clip. After 45 minutes of occlusion, the clip was removed and anti-OPN Ab (25 µg/mouse) or normal IgG isotype control (25 µg/mouse) was immediately administered intravenously. Blood, small intestine, and lung tissues were collected at 4 hours after reperfusion for various analyses. After intestinal I/R, mRNA and protein levels of OPN were significantly induced in the small intestine, lungs, and blood relative to sham-operated animals. Compared with the IgG control group, treatment of anti-OPN Ab significantly reduced plasma levels of pro-inflammatory cytokine and chemokine (IL-6 and MIP-2) and organ injury markers (AST, ALT, and LDH). The histological architecture of the gut and lung tissues in anti-OPN Ab-treated intestinal I/R-induced mice showed significant improvement versus the IgG control mice. The lung inflammation measured by the levels of IL-6, IL-1β, and MIP-2 was also significantly downregulated in the anti-OPN Ab-treated mice as compared with the IgG control mice. Besides, the lung MPO and neutrophil infiltration in anti-OPN Ab-treated mice showed significant reduction as compared with the IgG control animals. In

Address for correspondence, proofs, and reprint requests to: Ping Wang, MD, Chief Scientific Officer (CSO), Feinstein Institute for Medical Research, Professor and Vice Chairman for Research, Department of Surgery, Hofstra Northwell School of Medicine, 350 Community Dr., Manhasset, NY 11030, Tel: (516) 562-3411, Fax: (516) 562-2396, pwang@northwell.edu.

Conflicts of Interest

The authors have no financial conflicts of interest.

YH, MA designed the experiments. YH performed experiments and analyzed the data. MO, YH performed gut I/R model in mice. MA, WL-Y supervised the works. YH, MA prepared the manuscript. PW conceived the idea, reviewed the manuscript, managed and supervised the project. All authors have gone through and finally approved the manuscript for publication.

conclusion, we have demonstrated beneficial outcomes of anti-OPN Ab treatment in protecting against ALI, implicating a novel therapeutic potential in intestinal I/R.

Keywords

Osteopontin; Intestinal Ischemia-Reperfusion; Acute Respiratory Distress Syndrome; Inflammation; Neutrophil; Infiltration

INTRODUCTION

Intestinal ischemia-reperfusion (I/R) is associated with a variety of clinical conditions including acute mesenteric ischemia (AMI), volvulus, necrotizing colitis, trauma, hemorrhagic shock and intestinal transplant rejection (1–6). Despite huge clinical and scientific effort in this field, intestinal I/R remains critical challenge because of its high mortality rate as high as 60% to 80% (7, 8). Intestinal ischemia causes intestinal tissue hypoxia, inflammation such as cytokine and free radical production, and infiltration of neutrophils which results in intestinal mucosal barrier disruption and release of endotoxin into the circulation, leading to severe systemic inflammation and eventually multiple organ failure (MOF) (9). Especially, acute lung injury (ALI), clinically defined as acute respiratory distress syndrome (ARDS), is the primary complication during the sequential development of MOF (10). ARDS is characterized by an overproduction of pro-inflammatory cytokines, protein rich-edema fluid, hemorrhage and inactivation of surfactant in the lung tissues, contributing to an impairment of oxygenation (11). Therefore, development of effective therapies for intestinal I/R-induced ARDS is beneficial for patients with intestinal I/R injury and its related conditions.

Osteopontin (OPN) is a multifunctional glycoprotein originally isolated from bone. OPN is known to regulate biomineralization and remodeling in bone tissues (12). In contrast to its restricted distribution in normal tissues, OPN is strikingly upregulated at the sites of inflammation (13). In inflammatory condition, OPN plays diverse cellular functions in innate immune system starting from promoting T-helper cell type 1 (Th1) skewing and extends through the differentiation and proliferation of immune reactive cells (14–16). OPN also functions as a pro-inflammatory cytokine and recruits inflammatory cells to exaggerate tissue damage (17). Increased levels of OPN have been demonstrated in a variety of chronic inflammatory diseases (17–20), whereas the role of OPN in acute inflammatory diseases remains less elucidated.

Considering OPN as a pro-inflammatory molecule to exacerbate inflammation, we have recently demonstrated that blockade of OPN by its neutralizing antibody (anti-OPN Ab) attenuated systemic inflammation and protected mice from sepsis-induced ALI by inhibiting neutrophil infiltrations in lungs (21). However, its therapeutic efficacy in intestinal I/R remains unclear. Therefore, the current study was conducted to test the hypothesis that neutralization of OPN might attenuate intestinal I/R-induced systemic inflammation and ALI. Based on our current findings, mice treated with anti-OPN Ab attenuated intestinal I/R-induced ALI by reducing systemic inflammation and neutrophil infiltrations into the lung

tissues, implicating anti-OPN Ab as a potent therapeutic regimen against sterile inflammation.

MATERIALS AND METHODS

Animal model of intestinal I/R and administration of anti-OPN Ab

Eight-weeks-old male, C57BL/6 mice were purchased from Taconic (Albany, NY, USA). Animals were divided into three groups consisting of sham operation, intestinal I/R with normal goat IgG as isotype control (R&D Systems, Minneapolis, MN; Catalog No.: AB-108-C) administration, and intestinal I/R with affinity purified polyclonal goat anti-mouse OPN Ab (R&D Systems; Catalog No.: AF808) treatment. Intestinal I/R was induced by superior mesenteric artery (SMA) occlusion, as described previously (22). Briefly, mice were anesthetized with 2% isoflurane inhalation in 1 L of oxygen per minute. An upper midline laparotomy was performed to expose the abdomen and the SMA was isolated. Then the SMA was occluded with a vascular clip. On completion of 45 minutes of ischemia, the vascular clip was removed to allow reperfusion. At the beginning of reperfusion, mice were resuscitated with 500 μ l of normal saline subcutaneously (SC) and anti-OPN Ab (25 μ g/mouse) or equivalent volume and concentration of normal goat IgG isotype control was delivered by bolus injection into the tail vein. Afterward, the abdomen was closed and mouse was put back into the cage. Sham-operated animals underwent only midline laparotomy incision and closure, without intestinal ischemia or drug treatment. Four hours after reperfusion, animals were anesthetized again, and blood, small intestine and lung tissue samples were collected. Blood samples were centrifuged at 3000 g for 10 minutes to collect plasma. The plasma and tissue samples were frozen immediately in liquid nitrogen, and stored at -80° C until analysis. A section of small intestine with a similar area (proximal part of jejunum) and lung tissues were preserved in formalin for histopathological analysis. All experiments were performed in accordance with the guidelines for the use of experimental animals by the National Institutes of Health (Bethesda, MD) and were approved by the Institutional Animal Care and Use Committee of the Feinstein Institute for Medical Research (Manhasset, NY).

Measurement of OPN, pro-inflammatory cytokines and chemokine

Small intestine and lung tissues were homogenized in lysis buffer (10 mM Tris-HCl, pH 7.5, 120 mM NaCl, 1% NP-40, 1% sodium deoxycholate and 0.1% sodium dodecyl sulfate) containing a protease inhibitor cocktail (Roche Diagnostics, Indianapolis, IN). Protein concentration was determined by Bio-Rad protein assay reagent. Pro-inflammatory cytokines, interleukin-6 (IL-6) and IL-1 β in plasma and lung tissues were quantified by using the mouse ELISA kits (BD Biosciences, Franklin Lakes, NJ). Protein levels of OPN and macrophage inflammatory protein-2 (MIP-2) in plasma, intestine and lung tissues were measured by using the mouse ELISA kits (R&D Systems).

Histological examination

The small intestine and lung tissues were fixed in 10% formalin and then embedded in paraffin.

Later, the tissue blocks were cut into 5- μ m sections, placed onto glass slides and stained with hematoxylin-eosin (H&E), dehydrated, and mounted. Morphologic examinations in these tissues were evaluated by light microscopy in a blinded fashion. The severity of gut injury was scored from 0 to 4 by assessing villus-to-crypt ratio (normal ratio, 5:1), lymphocytic infiltrates, epithelial degeneration/necrosis, erosions, glandular dilatation, and transmural changes (23) by an experienced investigator. The severity of lung injury was also assessed by an experienced investigator using a scoring system as absent, mild, moderate, or severe injury (score 0 to 3, respectively) according to the following pathological features: 1) presence of exudates, 2) hyperemia/congestion, 3) intraalveolar hemorrhage/debris, 4) cellular infiltration, and 5) cellular hyperplasia, and a cumulative total histological injury score was calculated (24).

Immunostaining

For neutrophil staining, the 10% formalin-fixed, paraffin-embedded lung tissues were dewaxed in xylene and rehydrated in a graded series of ethanol. The slides were heated in 0.92% citric acid buffer (Vector, Burlingame, CA) at 95° C for 30 minutes. After cooling to room temperature, the slides were incubated with 2% H₂O₂ in 60% methanol and blocked in 2% normal rabbit serum/Tris-buffered saline. Anti-Gr-1 antibody (BioLegend, San Diego, CA) was then applied and incubated overnight. Vectastain ABC reagent and DAB kit (Vector) were used to reveal the immunohistochemical reaction. Slides were counterstained with 4, 6-diamidino-2-phenylindole and examined under a phase contrast light microscope (Eclipse Ti-S; Nikon, Melville, NY).

Real-time quantitative reverse transcription-PCR (qRT-PCR)

Total RNA was extracted from lung tissues by using TRIzol (Invitrogen, Carlsbad, CA) and was reverse-transcribed into cDNA using reverse transcriptase (Applied Biosystems, Foster City, CA). A Polymerase chain reaction (PCR) was carried out in 25 μ l of final volume containing 0.1 μ M of each forward and reverse primer, cDNA and 12.5 μ l SYBR Green PCR Master Mix (Life Technologies, Grand Island, NY). Amplification was conducted using an Applied Biosystems 7300 real-time PCR machine under the thermal profile of 50°C for 2 min, 95°C for 10 min followed by 45 cycles of 95°C for 15 seconds and 60°C for 1 min. For relative quantization, 2^{-ddCt} method normalized to mouse β -actin mRNA was used. Relative expression of mRNA was expressed as the fold change in comparison with the tissues of sham-operated animals. The primers used for this study were: OPN(NM_001204201) Forward: TCTGATGAGACCGTCACT GC, Reverse: AGGTCCTCATCT GTGGCATC; IL-6(NM_031168) Forward: CCGGAGAGGA GACTTCACAG, Reverse: GGAAATTGGGGTAGGAAGGA; IL-1 β (NM_008361)Forward: C AGGATGAGGACATGAGCACC, Reverse: CTCTGCAGACTCAAACCTCCAC; MIP-2(NM_009140) Forward: CCCTGGTTCAGAAAATCATCCA, Reverse: GCTCCTCCTT TCCAGGT CAGT; β -actin(NM_007393)Forward: CGTGAAAAGATGACCCAGATCA, Reverse: TGG TACGACCAGAGGCATACAG.

Statistical analysis

Data are expressed as mean \pm standard error of the mean (SEM) and analyzed using Sigma Plot11 graphing and statistical analysis software (Systat Software Inc., San Jose, CA, USA).

Multiple groups were compared by one-way analysis of variance (ANOVA) using the Student-Newman-Keuls' (SNK) test. Student's t test was used for two-group analysis. Differences in values were considered significant if $p < 0.05$.

RESULTS

OPN is increased in the gut, lung, and blood after intestinal I/R

To determine the status of OPN expression at its mRNA and protein levels after intestinal I/R, the gut and lung tissues of sham-operated mice and intestinal I/R-induced mice were subjected for real-time qRT-PCR and ELISA, respectively. In the gut tissues, the mRNA and protein expression of OPN were significantly upregulated by 130 and 120 % in intestinal I/R-induced mice as compared to the sham-operated animals, respectively (Fig 1A). Similarly, in the lung tissues, the mRNA and protein expression of OPN in intestinal I/R group were significantly increased by 110 and 50 % as compared to the sham-operated group, respectively (Fig 1B). Moreover, the alteration of OPN expression after intestinal I/R in plasma was investigated by ELISA, which showed elevated levels of OPN in the intestinal I/R group by 130 % as compared to the sham-operated group (Fig 1C).

Neutralization of OPN decreases blood levels of organ injury and inflammatory markers after intestinal I/R

Clinical markers such as AST, ALT, and LDH in blood were measured at 4 hours after intestinal I/R in mice to assess the severity of organ injury. Compared to the sham-operated group, the levels of AST, ALT and LDH were significantly elevated in IgG isotype control group (Figs 2A–C). In contrast, the treatment with anti-OPN Ab significantly reduced the levels of these injury markers in plasma by 26%, 53%, and 41%, respectively, as compared to the IgG control group (Figs 2A–C). We have also examined the effect of anti-OPN Ab treatment on systemic levels of pro-inflammatory cytokine, IL-6 and chemokine, MIP-2. The plasma levels of IL-6 and MIP-2 were significantly increased in IgG control group as compared to the sham-operated group, whereas treatment with anti-OPN Ab markedly decreased the plasma levels of IL-6 by 48% and MIP-2 by 64% as compared to the IgG control group (Figs 2D, E).

Treatment with anti-OPN Ab ameliorates gut tissue injury after intestinal I/R

Macroscopic appearance of the intestine after I/R-induced injury exhibited severe tissue necrosis, edema, and ischemic darkness with vascular congestion throughout the tissue in comparison with the sham-operated group (Fig 3A). However, the treatment of anti-OPN Ab greatly reduced the severity of macroscopic appearance of intestinal damage such as necrosis and ischemic congestion (Fig 3A). In examination of the histopathological changes, severe mucosal damage with decreased villus height, epithelial cell necrosis, increased numbers of lymphocytes and plasma cells in lamina propria, and glandular destruction were microscopically observed in the gut tissues after I/R in comparison with the sham-operated group (Fig 3B). On the other hand, the integrity of morphological structure was much well preserved in the intestine of anti-OPN Ab-treated group when compared with the IgG isotype control-treated group (Fig 3B). As quantified in Fig 3C, animals underwent intestinal I/R with IgG control treatment exhibited a dramatic increase in histological injury score of

the intestinal tissue when compared to the sham-operated animals, which was reduced significantly with administration of anti-OPN Ab.

Administration of anti-OPN Ab inhibits pro-inflammatory cytokines and chemokine expression in the lung tissues after intestinal I/R

We examined the expression of pro-inflammatory cytokines and chemokine in the lung tissues at their mRNA and protein levels by real-time qRT-PCR and ELISA, respectively, to assess the local inflammation in the lung tissues after intestinal I/R. Both the mRNA and protein levels of IL-6 in the lung tissues were significantly increased in the IgG control group as compared to the sham-operated group (Fig 4A). However, the treatment with anti-OPN Ab significantly inhibited its mRNA and protein levels by 77% and 51%, respectively, as compared to the IgG control group (Fig 4A). Similarly, the expression levels of IL-1 β in both mRNA and proteins in the lung tissues were significantly upregulated in the IgG control group as compared to the sham-operated group, whereas the treatment with anti-OPN Ab significantly reduced its mRNA and protein levels by 77% and 40%, respectively, relative to the IgG control group (Fig 4B). Beside these inflammatory markers, both the mRNA and protein levels of MIP-2 in the lung tissues were significantly upregulated in the IgG control group as compared to the sham-operated group and they were significantly decreased in anti-OPN Ab-treated animals by 86% and 28%, respectively, relative to the IgG control-treated intestinal I/R-induced mice (Fig 4C).

Treatment of anti-OPN Ab improves lung histology after intestinal I/R in mice

To assess the effect of neutralizing OPN Ab therapy on the lung injury caused by intestinal I/R, histological examination of lung tissues were performed and the severity of injury was graded with an established scoring system as described in the Materials and Methods. Representative histological architectures of the sham-operated, IgG control, and anti-OPN Ab-treated mice are shown in Fig 5A. The lung tissues from the IgG control group presented substantial morphological changes including edema, hemorrhage/congestion, alveolar collapse, and inflammatory cell infiltrations in comparison with the sham-operated group. By contrast, administration of anti-OPN Ab dramatically attenuated this histological deterioration when compared to the IgG control group. As quantified in Fig 5B, the lung tissue in the IgG group showed a significant increase in the histological injury score as compared to the sham-operated group, whereas the treatment with anti-OPN Ab significantly reduced the lung histological injury score by 30% as compared to IgG control group.

Neutralization of OPN reduces neutrophil infiltration and MPO activity in the lungs after intestinal I/R-mediated injury

The lung tissues collected at 4 hours after intestinal I/R were immunostained with anti-Gr-1 Ab, a surface marker of activated neutrophils, to assess the effect of anti-OPN Ab treatment on neutrophil infiltration. As shown in Fig 6A, the presence of Gr-1-positive cells in the lung tissues was dramatically higher in the IgG control group as compared to the sham-operated animals. However, there were considerably lower numbers of Gr-1 positive cells in the OPN Ab-treated group than the IgG control group mice with intestinal I/R-mediated injuries. Furthermore, the tissue damage in ALI is also linked with the MPO activity within the lung

tissues. The MPO activity in the lung tissues harvested at 4 hours after intestinal I/R was significantly increased in the IgG control group as compared to the sham-operated animals, whereas the treatment with anti-OPN Ab significantly reduced its activity by 60% in comparison with the IgG control group (Fig 6B).

DISCUSSION

Osteopontin is produced by immune-reactive cells, which include activated T cells, dendritic cells, and macrophages to play critical roles in innate and adaptive immune systems (25, 26). Several noteworthy functions of OPN have been reported so far, such as its chemoattractant property to enhance the migration of immune competent cells towards the site of inflammation (14, 21). OPN is also known to promote T cell proliferation and macrophage differentiation by its novel interaction with integrins and CD44 receptors (15, 17, 27). Besides these functions, OPN has also been shown to regulate IFN- γ and IL-17 production and dampen IL-10 production by T cells (15). Based on these pro-inflammatory functions, OPN is therefore considered as a pro-inflammatory molecule and have been well investigated in a wide range of chronic inflammatory diseases (17–20). In contrast to its chronic pathophysiological role, current literatures show inadequate evidence on its role in acute inflammatory diseases, even though a few studies were carried-out in non-sterile inflammatory disease conditions, like polymicrobial sepsis, and *Pneumococcal pneumonia* infections (28–30). Therefore, dealing with the elucidation of the role of OPN in sterile and acute inflammation will enhance our understanding towards implementing OPN as a novel therapeutic target in a wide range of inflammatory diseases.

By using OPN knock-out mice, Van der Windt *et al* have demonstrated reduced plasma levels of pro-inflammatory cytokines and chemokines in *Streptococcus pneumonia* infected animals (28). In the same way but adopting more clinically relevant approach, our recent study has also clearly demonstrated the protective role of OPN neutralizing Ab against sepsis-induced ALI in mice by inhibiting exaggerated inflammatory responses and neutrophil infiltrations in lungs through the modulation of MAP kinase pathway (21). Similar to sepsis, I/R injuries of several organs can be accompanied by a systemic inflammatory response as well as neutrophil infiltrations into remote organs. It is therefore conceivable that OPN may play a deleterious role in I/R-mediated organ injuries. In support of this notion, Zhang *et al* have revealed that OPN expression was increased in renal tubular epithelial cells after renal I/R in mice, which resulted in exaggerated initial inflammatory responses as mediated by the NK cell activation (31). In contrast to renal ischemia model, recent study has also demonstrated an upregulation of OPN expression in the liver tissues and plasma after hepatic I/R which were shown to play protective functions in hepatic injury and inflammation by its ability to partially prevent death of hepatocytes and to limit the production of toxic inducible nitric oxide synthase (iNOS)-derived nitric oxide (NO) by macrophages (32). Thus, the data from the above studies may suggest that OPN might play dual roles depending on ischemia and reperfusion models adopted in various organs. Therefore, extensive studies on OPN could be helpful to clearly define its potential role in various I/R-mediated tissue injuries. Interestingly, our study utilizing murine intestinal ischemia-reperfusion model revealed dramatic upregulation of OPN levels in gut, lungs, and systemic circulation which resulted in exaggerated systemic inflammation causing local and

remote organ injuries if its function is not abrogated immediately after ischemia. Therefore, identification of the status of OPN expression and its function in intestinal I/R is novel and implicates an emerging therapeutic tool in murine experimental intestinal I/R.

In the current study, we induced intestinal I/R in mice by the occlusion of superior mesenteric artery (SMA) using the vascular clip and administered the drug immediately after reperfusion. Among various clinical situations complicated with intestinal I/R (1–6), our model of intestinal I/R is most relevant to acute mesenteric ischemia (AMI). Although the treatment option for AMI is mainly focused on surgical method, some patients may be good candidates for thrombolytic therapy, which enables the administration of drugs at the same time as reperfusion possible. Besides, the treatment with fluid resuscitation in intestinal I/R without mechanic occlusion of intestinal vessels such as trauma or hemorrhagic shock could be the timing of reperfusion of intestine. But it is pretty sure that the timing of drug administration should be more investigated in the future. The lack of late time points in terms of treatment is considered to be the limitation of our current study.

It has been well recognized that the damage of intestinal mucosal barrier after intestinal IR may promote the translocation of bacteria into the circulation as well as into other organs such as lung tissues (33). The lung is the most susceptible remote organ to be injured after intestinal I/R (10). Neutrophils play a central role in innate immune responses to eradicate microbial infections (34). However, excessive and prolonged neutrophil infiltration into the lungs results in the overwhelming release of cytokines and other pro-inflammatory mediators, causing consequent increase of endothelial and epithelial permeability, fluid and protein extravasation, and pulmonary capillary endothelial cell injury and finally severe lung tissue injury (35). Our current findings showed that intestinal I/R increased lung neutrophil infiltration and local cytokine, chemokine and MPO production, which were reversed back towards normal levels by treating the intestinal I/R animals with anti-OPN Ab, which ultimately led to controlled release of pro-inflammatory mediators from neutrophils. Of note, we previously reported recombinant OPN (rOPN) to promote neutrophil migration *in vitro* through the activation and phosphorylation of focal adhesion kinase (FAK) and MAP kinases as plausible upstream and downstream mediators of this event, respectively (21). In support of this *in vitro* finding, we also provided direct *in vivo* evidence of OPN-mediated neutrophil migration in lung after intra-tracheal administration of rOPN in mice. Since one of the hallmark features of intestinal I/R-mediated injury is to promote exaggerated neutrophil accumulation in lung to cause ALI (35), we therefore anticipated that inhibition of neutrophil infiltration in the lung tissues could be the key mechanism of beneficial effect of anti-OPN Ab treatment in the intestinal I/R-induced ALI. However, we cannot rule-out the possibility that other potential mechanism of anti-OPN Ab treatment mediated inhibition of ALI. In addition, our current study doesn't delineate the localization of OPN during intestinal I/R, which might allow us some speculation as to mechanisms of action of OPN. Further study in this field of interest would provide additional information to help support the clinical outcome of anti-OPN Ab treatment in intestinal I/R.

CONCLUSIONS

We have demonstrated the beneficial outcomes of anti-OPN Ab treatment in intestinal IR model in mice by revealing the maintained histological integrity, attenuated neutrophil chemotaxis and infiltrations, and decreased pro-inflammatory cytokines and chemokine levels in lungs. These data strongly implicate that anti-OPN Ab could be a novel therapeutic potential in intestinal I/R-mediated ARDS.

Acknowledgments

Source of Funding

This study was supported by the National Institutes of Health (NIH) grants, GM053008, GM057468, and HL076179 (PW).

ABBREVIATIONS

I/R	ischemia-reperfusion
AMI	acute mesenteric ischemia
MOF	multiple organ failure
ALI	acute lung injury
ARDS	acute respiratory distress syndrome
OPN	osteopontin
SMA	superior mesenteric artery
MIP-2	macrophage inflammatory protein-2
iNOS	inducible nitric oxide synthase
NO	nitric oxide
FAK	focal adhesion kinase
MAP kinase	mitogen activated protein kinase
rOPN	recombinant osteopontin.

REFERENCES

1. Yasuhara H. Acute mesenteric ischemia: the challenge of gastroenterology. *Surg Today*. 2005; 35:185–195. [PubMed: 15772787]
2. Schwartz MZ. Novel therapies for the management of short bowel syndrome in children. *Pediatr Surg Int*. 2013; 29:967–974. [PubMed: 23989526]
3. Nankervis CA, Giannone PJ, Reber KM. The neonatal intestinal vasculature: contributing factors to necrotizing enterocolitis. *Semin Perinatol*. 2008; 32:83–91. [PubMed: 18346531]
4. Corcos O, Nuzzo A. Gastro-intestinal vascular emergencies. *Best Pract Res Clin Gastroenterol*. 2013; 27:709–725. [PubMed: 24160929]

5. Fishman JE, Sheth SU, Levy G, Alli V, Lu Q, Xu D, Qin Y, Qin X, Deitch EA. Intraluminal nonbacterial intestinal components control gut and lung injury after trauma hemorrhagic shock. *Ann Surg.* 2014; 260:1112–1120. [PubMed: 24646554]
6. Mallick IH, Yang W, Winslet MC, Seifalian AM. Ischemia-reperfusion injury of the intestine and protective strategies against injury. *Dig Dis Sci.* 2004; 49:1359–1377. [PubMed: 15481305]
7. Acosta S. Epidemiology of mesenteric vascular disease: clinical implications. *Semin Vasc Surg.* 2010; 23:4–8. [PubMed: 20298944]
8. Higuchi S, Wu R, Zhou M, Marini CP, Ravikumar TS, Wang P. Gut hyperpermeability after ischemia and reperfusion: attenuation with adrenomedullin and its binding protein treatment. *Int J Clin Exp Pathol.* 2008; 1:409–418. [PubMed: 18787625]
9. Eltzschig HK, Eckle T. Ischemia and reperfusion - from mechanism to translation. *Nat Med.* 2011; 17:1391–1401. [PubMed: 22064429]
10. Mura M, Andrade CF, Han B, Seth R, Zhang Y, Bai XH, Waddell TK, Hwang D, Keshaviee S, Liu M. Intestinal ischemia-reperfusion-induced acute lung injury and oncotic cell death in multiple organs. *Shock.* 2007; 28:227–238. [PubMed: 17666944]
11. Jesu's Villar: What is the acute respiratory distress syndrome? *Respir Care.* 2011; 56(10):1539–1545. [PubMed: 22008395]
12. Choi ST, Kim JH, Kang EJ, Lee SW, Park MC, Park YB, Lee SK. Osteopontin might be involved in bone remodeling rather than in inflammation in ankylosing spondylitis. *Rheumatology.* 2008; 47(12):1775–1779. [PubMed: 18854347]
13. Liaw L, Birk DE, Ballas CB, Whitsitt JS, Davidson JM, Hogan BL. Altered wound healing in mice lacking a functional osteopontin gene (spp1). *J Clin Invest.* 1998; 101(7):1468–1478. [PubMed: 9525990]
14. Ashkar S, Weber GF, Panoutsakopoulou V, Sanchirico ME, Jansson M, Zawaideh S, Rittling SR, Denhardt DT, Glimcher MJ, Cantor H. Eta-1(osteopontin); an early component of type-1 (cell mediated) immunity. *Science.* 2000; 287(5454):860–864. [PubMed: 10657301]
15. Murugaiyan G, Mittal A, Weiner HL. Increased osteopontin expression in dendritic cells amplifies IL-17 production by CD4+ T cells in experimental autoimmune encephalomyelitis and in multiple sclerosis. *J Immunol.* 2008; 181(11):7480–7488. [PubMed: 19017937]
16. Nystrom T, Duner P, Hultgardh-Nilsson A. A constitutive endogenous osteopontin production is important for macrophage function and differentiation. *Exp Cell Res.* 2007; 313(6):1149–1160. [PubMed: 17306792]
17. Lund SA, Giachelli CM, Scatena M. The role of osteopontin in inflammatory processes. *J Cell Commun Signal.* 2009; 3:311–322. [PubMed: 19798593]
18. El-Tanani MK, Campbell FC, Kurisetty V, Jin D, McCann M, Rudland PS. The regulation and role of osteopontin in malignant transformation and cancer. *Cytokine Growth Factor Rev.* 2006; 17(6):463–474. [PubMed: 17113338]
19. Comabella M, Pericot I, Goertsches R, Nos C, Castillo M, Blas Navarro J, Rio J, Montalban X. Plasma osteopontin levels in multiple sclerosis. *J Neuroimmunol.* 2005; 158(1–2):231–239. [PubMed: 15589058]
20. Aziz MM, Ishihara S, Mishima Y, Oshima N, Moriyama Y, Yuki T, Kadowaki Y, Rumi MA, Amano Y, Kinoshita Y. MFG-E8 attenuates intestinal inflammation in murine experimental colitis by modulating osteopontin-dependent alphavbeta3 integrin signaling. *J Immunol.* 2009; 182(11):7222–7232. [PubMed: 19454719]
21. Hirano Y, Aziz M, Yang WL, Wang Z, Zhou M, Ochani M, Khader A, Wang P. Neutralization of osteopontin attenuates neutrophil migration in sepsis-induced acute lung injury. *Crit Care.* 2015; 19:53. [PubMed: 25887405]
22. Cui T, Miksa M, Wu R, Komura H, Zhou M, Dong W, Wang Z, Higuchi S, Chaung W, Blau SA, Marini CP, Ravicumar TS, Wang P. Milk fat globule epidermal growth factor 8 attenuates acute lung injury in mice after intestinal ischemia and reperfusion. *Am J Respir Crit Care Med.* 2010; 181:238–246. [PubMed: 19892861]
23. Stallion A, Kou TD, Latifi SQ, Miller KA, Dahms BB, Dudgeon DL, Levine AD. Ischemia/reperfusion: a clinically relevant model of intestinal injury yielding systemic inflammation. *J Pediatr Surg.* 2005; 40:470–477. [PubMed: 15793720]

24. Bachofen M, Weibel ER. Structural alterations of lung parenchyma in the adult respiratory distress syndrome. *Clin Chest Med.* 1982; 3:35–56. [PubMed: 7075161]
25. Wang KX, Denhardt DT. Osteopontin, role in immune regulation and stress responses. *Cytokine Growth Factor Rev.* 2008; 19:333–345. [PubMed: 18952487]
26. Cantor H, Shinohara ML. Regulation of T-helper-cell lineage development by osteopontin, the inside story. *Nat Rev Immunol.* 2009; 9:137–141. [PubMed: 19096390]
27. Weber GF, Zawaideh S, Hikita S, Kumar VA, Cantor H, Ashkar S. Phosphorylation-dependent interaction of osteopontin with its receptors regulates macrophage migration and activation. *J Leukoc Biol.* 2002; 72(4):752–761. [PubMed: 12377945]
28. Van der Windt GJW, Hoogendijk AJ, Schouten M, Hommes TJ, de Vos AF, Florguin S, van der Poll T. Osteopontin impairs host defense during pneumococcal pneumonia. *J Infect Dis.* 2011; 203:1850–1858. [PubMed: 21606543]
29. Van der Windt GJW, Wiersinga WJ, Wieland CW, Tjia IC, Day NP, Peacock SJ, Florguin S, van der Poll T. Osteopontin impairs host defense during established gram-negative sepsis caused by burkholderia pseudomallei (melioidosis). *PLoS Negl Trop Dis.* 2010; 4(8):e806. [PubMed: 20824216]
30. Vaschetto R, Nicola S, Olivieri C, Boggio E, Piccolella F, Mesturini R, Damnotti F, Colombo D, Navalesi P, Della Corte F, Dianzani U, Chiocchetti A. Serum levels of osteopontin are increased in SIRS and sepsis. *Intensive Care Med.* 2008; 34:2176–2184. [PubMed: 18807011]
31. Zhang ZX, Shek K, Wang S, Huang X, Lau A, Yin Z, Sun H, Liu W, Garcia B, Rittling S, Jevnikar AM. Osteopontin expressed in tubular epithelial cells regulates NK cell-mediated kidney ischemia reperfusion injury. *J Immunol.* 2010; 185(2):967–973. [PubMed: 20548025]
32. Patouraux S, Rousseau D, Rubio A, Bonnafous S, Lavallard VJ, Lauron J, Saint-Paul MC, Bailly-Maitre B, Tran A, Crenesse D, Gual P. Osteopontin deficiency aggravates hepatic injury induced by ischemia-reperfusion in mice. *Cell Death Dis.* 2014; 5:e1208. [PubMed: 24810044]
33. Koury J, Deitch EA, Homma H, Abungu B, Gangurde P, Condon MR, Lu Q, Xu DZ, Feinman R. Persistent HIF-1alpha activation in gut ischemia/reperfusion injury: potential role of bacteria and lipopolysaccharide. *Shock.* 2004; 22:270–277. [PubMed: 15316398]
34. Araham E. Neutrophils and acute lung injury. *Crit Care Med.* 2003; 31:195–199. [PubMed: 12545015]
35. Schmeling DJ, Caty MG, Oldham KT, Guice KS, Hinshaw DB. Evidence for neutrophil related acute lung injury after intestinal ischemia-reperfusion. *Surgery.* 1989; 106:195–201. [PubMed: 2763027]

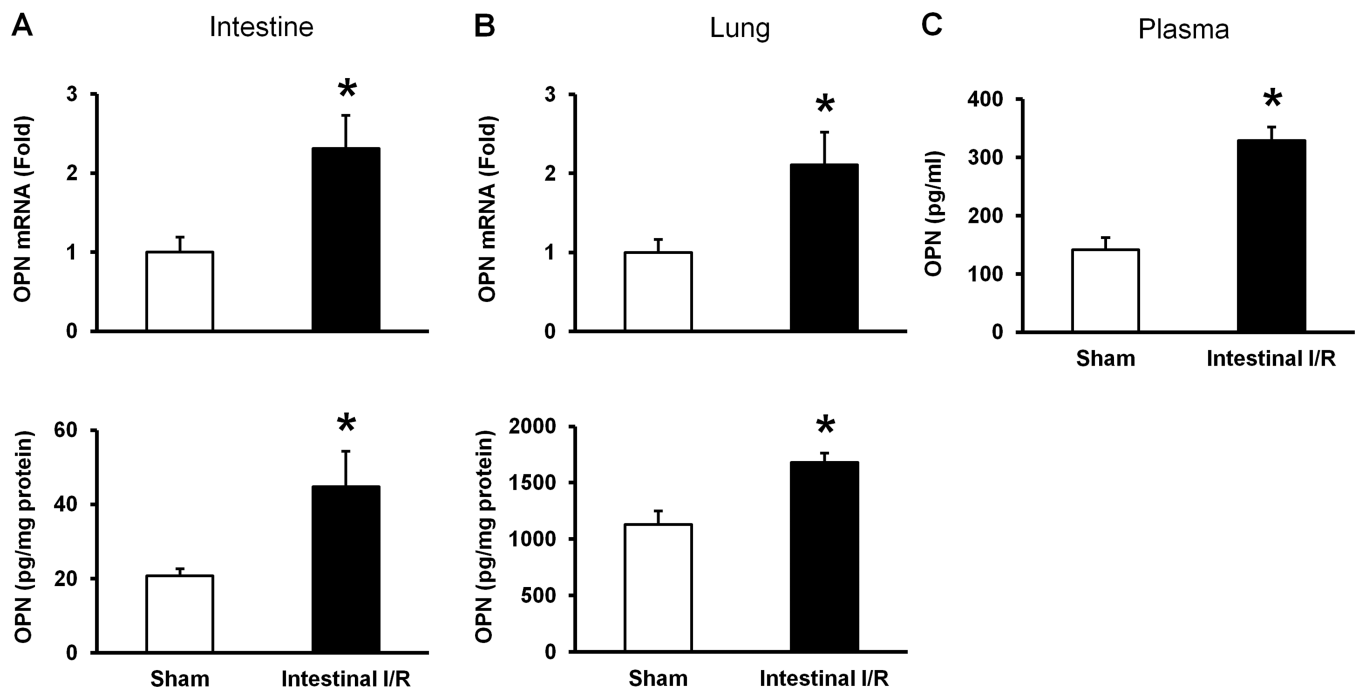


Figure 1. Expression of OPN in intestine, lungs and plasma after intestinal I/R in mice Intestine, lungs and blood samples were harvested 4 hours after intestinal ischemia reperfusion or sham operation. Expression of OPN in intestine (**A**) and lung (**B**) at its mRNA and protein levels was measured by using real-time qRT-PCR and ELISA, respectively. Gene expression of OPN at its mRNA levels was normalized to β -actin and the sham expression level was designated as one for comparison. (**C**) OPN level in plasma was measured by ELISA. Data are expressed as means \pm SE (n = 4–9 mice/group) and compared by *Student's t test* (*p < 0.05 vs. sham-operated animals).

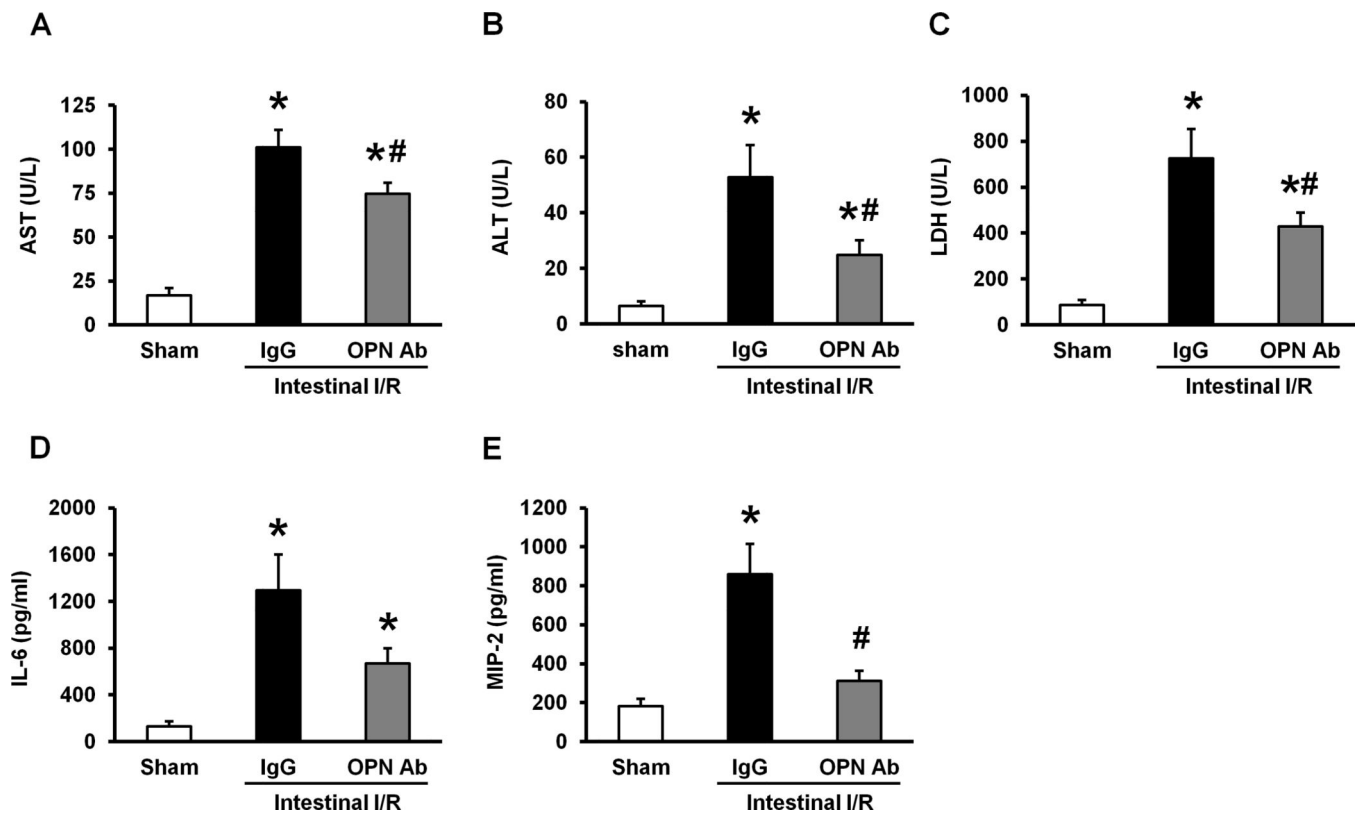


Figure 2. Effect of anti-OPN Ab treatment on plasma levels of organ injury markers and pro-inflammatory cytokine and chemokine in intestinal I/R mice

Blood samples were drawn at 4 hours after intestinal ischemia reperfusion of sham-operated, IgG and anti-OPN Ab-treated mice for measuring (A) AST, (B) ALT, and (C) LDH.

Similarly, the plasma samples collected at 4 hours after reperfusion were measured for (D) IL-6, and (E) MIP-2 by ELISA. Data are expressed as means \pm SE (n = 7–8 mice/group) and compared by one-way ANOVA and SNK method (*p < 0.05 vs. sham-operated group; #p < 0.05 vs. IgG control).

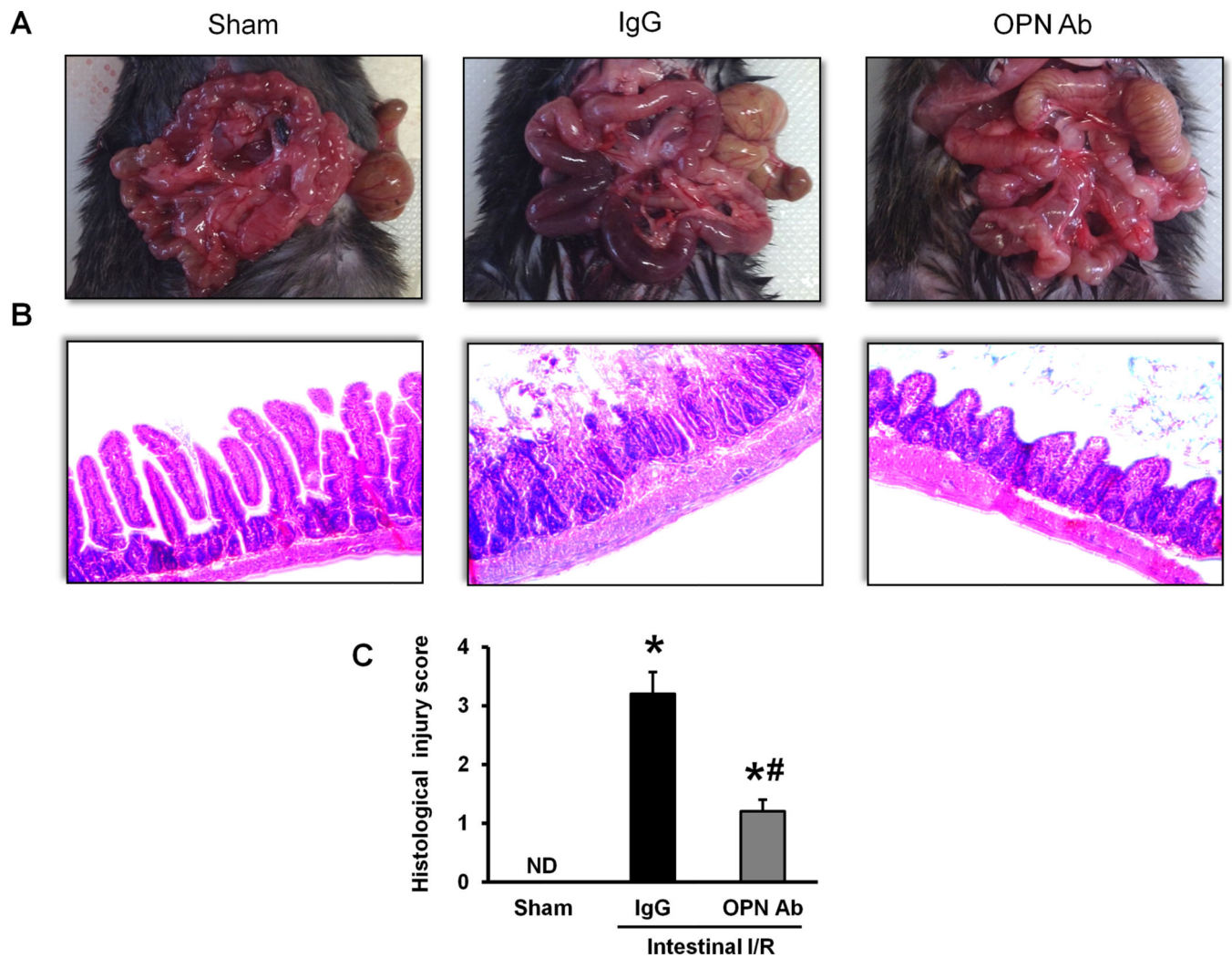


Figure 3. Alterations of intestinal morphology after intestinal I/R in mice

(A) Representative images for the gross morphological appearance of the intestine at 4 hours after intestinal ischemia reperfusion from sham-operated, IgG and anti-OPN Ab-treated mice are shown. (B) Intestinal tissues harvested at 4 hours after intestinal ischemia reperfusion were stained with H&E, and examined under light microscopy at 200 \times original magnifications. Representative images for the sham-operated group, IgG and anti-OPN Ab treatment groups are shown. (C) Histological injury scores of the intestine in different groups were quantified as described in Materials and methods. Data are expressed as mean \pm SE (n = 5/group) and compared by one-way ANOVA and SNK method (*p < 0.05 vs. sham-operated mice; #p < 0.05 vs. IgG control). ND, not detectable.

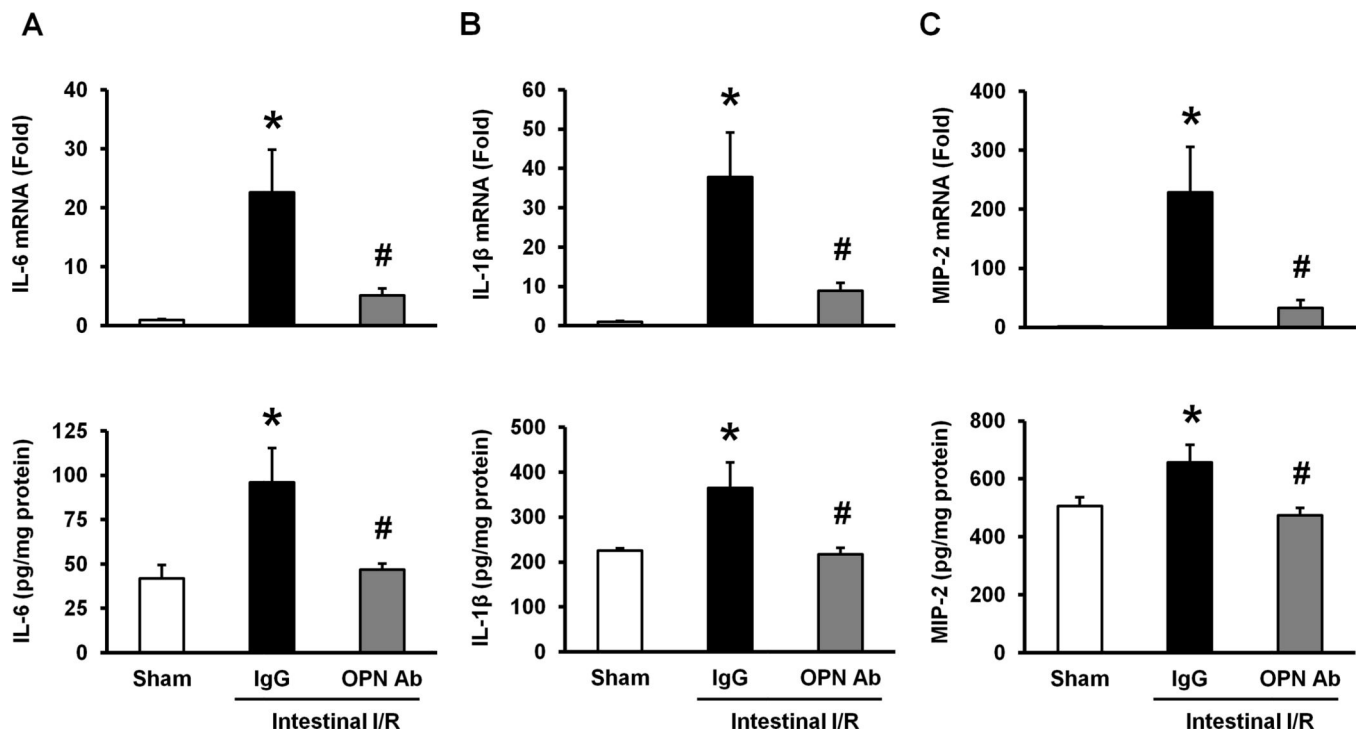


Figure 4. Effect of anti-OPN Ab on the expression of pro-inflammatory cytokines and chemokine in the lungs after intestinal I/R in mice

Lung tissues were collected at 4 hours after intestinal ischemia reperfusion from sham-operated, IgG and anti-OPN Ab-treated mice. The tissue expression of (A) IL-6, (B) IL-1 β and (C) MIP-2 at its mRNA and protein levels was measured by using real-time qRT-PCR and ELISA, respectively. Gene expression was normalized to β -actin. The sham expression level was designated as one for comparison. Data are represented as means \pm SE (n = 5–10 mice/group) and compared by one-way ANOVA and SNK method (*p < 0.05 vs. sham-operated animals; #p < 0.05 vs. IgG control).

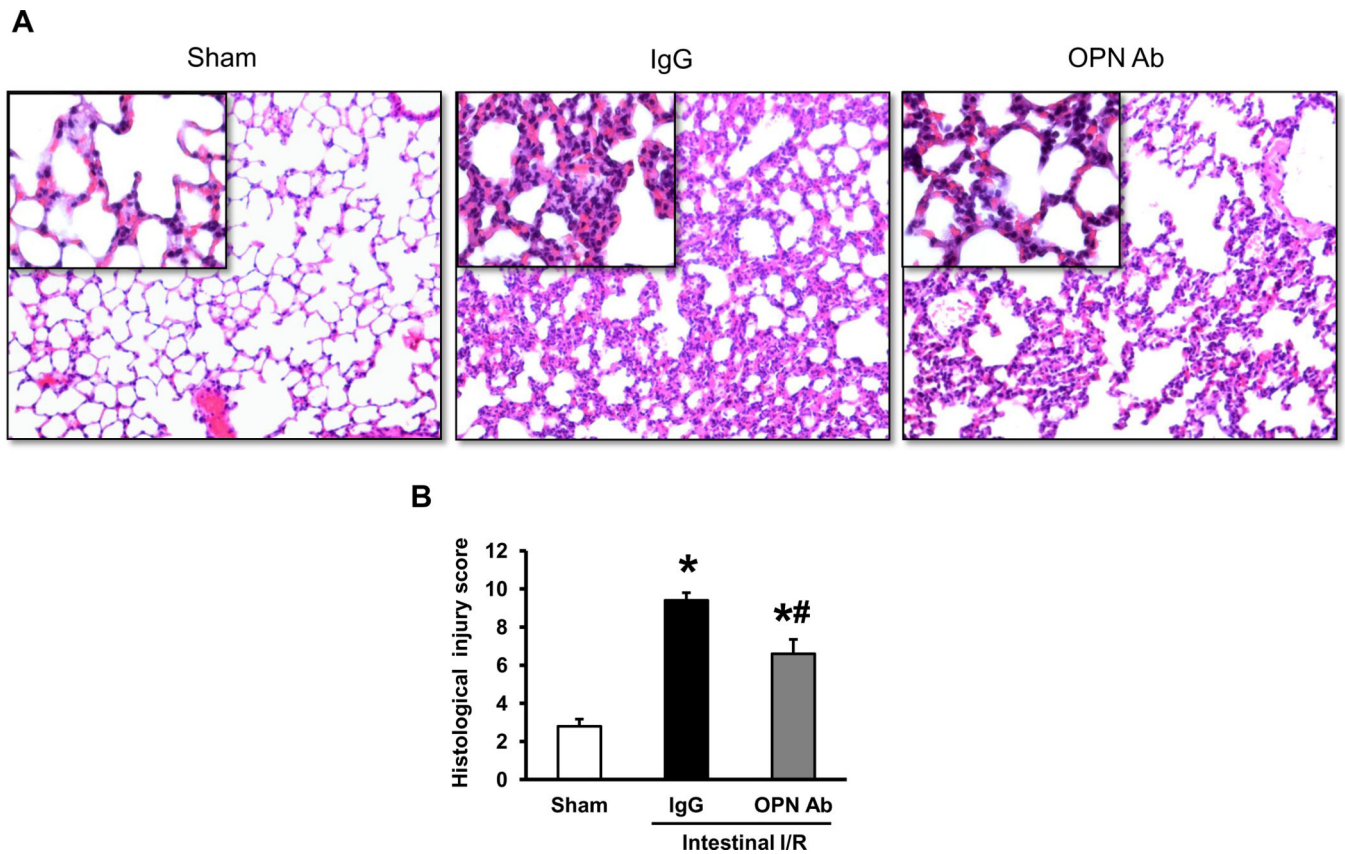


Figure 5. Evaluation of lung histology after intestinal I/R in mice
(A) Lung tissues harvested at 4 hours after intestinal ischemia reperfusion were stained with H&E, and examined under light microscopy at 200× original magnifications (inset: ×400 original magnifications). Representative images for the sham-operated, IgG and anti-OPN Ab treatment groups are shown. **(B)** Histological injury scores of the lungs in different groups were quantified as described in the materials and methods. Data are expressed as means ± SE (n = 5 mice/group) and compared by one-way ANOVA and SNK method (*p < 0.05 vs. sham-operated group; #p < 0.05 vs. IgG control).

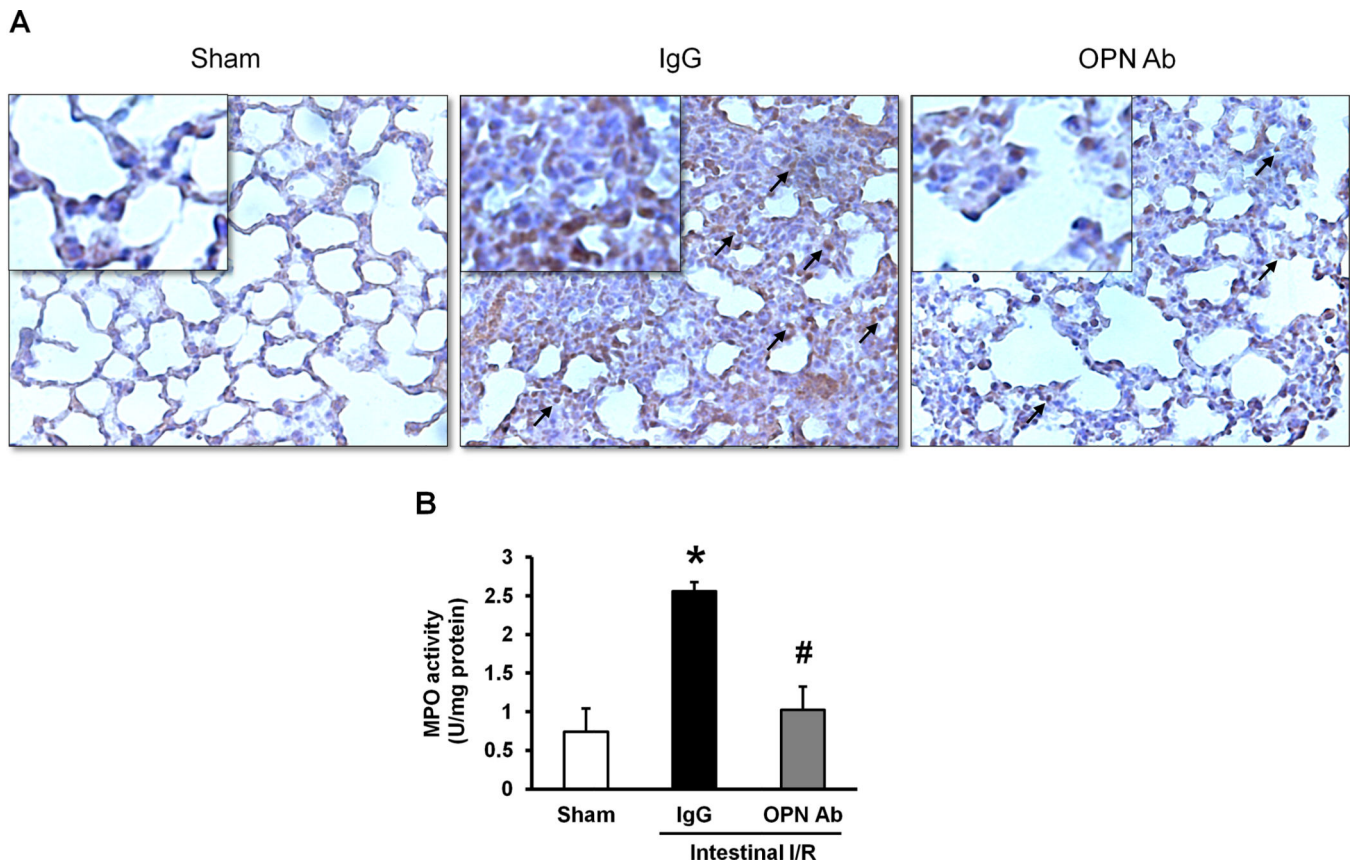


Figure 6. Assessment of neutrophil infiltration into the lungs after intestinal I/R
(A) Lung tissues harvested at 4 hours after intestinal ischemia reperfusion were immunostained against Gr-1 and examined under light microscopy at 200 \times original magnifications (inset: \times 400 original magnification). Representative images for the sham-operated animals, IgG and anti-OPN Ab treatment groups are shown. Arrows indicate examples of areas of staining Gr-1 positive cells. **(B)** Myeloperoxidase (MPO) activities in lung tissues were determined spectrophotometrically. Data are expressed as means \pm SE (n = 4–5 mice/group) and compared by one-way ANOVA and SNK method (*p < 0.05 vs. sham-operated animals; #p < 0.05 vs. IgG control).